RSC Advances

PAPER

View Article Online
View Journal | View Issue

Cite this: *RSC Adv.*, 2014, **4**, 65044

Isothiocyanato and azido coordination induced structural diversity in zinc(II) complexes with Schiff base containing tetrahydrofuran group: synthesis, characterization, crystal structure and fluorescence study†

Haridas Mandal, Sukanta Chakrabartty and Debashis Ray*

Three new structurally diverse zinc(II) complexes of formula $[H_3O][ZnL_2]ClO_4$ (**1**), $[Zn_2(\mu\text{-}L)_2(NCS)_2]$ (**2**) and $[Zn_3(\mu\text{-}L)_2(\mu\text{-}N_3)_4]_n$ (**3**) have been synthesized using the same furan-based tridentate ONO-donor Schiff base ligand HL (2-hydroxybenzyl-2-tetrahydrofurylmethyl)imine and characterized by X-ray structural analysis. Complex **1** is mononuclear, whereas **2** is a double phenoxido-bridged dinuclear compound. The novel polymeric compound **3** from azido coordination driven aggregation possesses a very rare 1D structure in which the dinuclear ligand-bound Zn_2L_2 fragments are bridged by four ligand-free $\mu_{1,1}$-azido bridging $Zn(N_3)_4^{2-}$ units resulting in a zigzag arrangement of repeating triangular Zn_3 motifs with structural similarity to the P1 nuclease. Solid state mixing and grinding processes were applied for the ligand exchange reaction and core conversion. In mechanochemical solvent free synthetic routes **1** reacts with isothiocyanato and azido ions to provide **2** and **3** in pure form. The ligand HL serves as sensitive fluorescent probe for Zn^{2+}, and complex **1** for SCN^- and N_3^- ions in MeOH medium. Coordination induced fluorescence enhancement due to intraligand $\pi \rightarrow \pi^*$ transition in the presence of Zn^{2+} of HL and quenching of emission intensities of **1** with SCN^- and N_3^- anions are accounted for by the formation of hitherto unknown complexes [Zn(L)(X)] (where X = ClO_4^-, SCN^- and N_3^-). HL shows chelation-enhanced fluorescence response from strong metal ion coordination and binding of isothiocyanato and azido anions with an appreciable lifetime of the fluorophore signals. Excitation at 380 nm of MeOH solutions of all three complexes in air exhibit excited state life-time spanning from 2.5–4.8 ns.

Received 27th September 2014
Accepted 21st November 2014

DOI: 10.1039/c4ra11352g

www.rsc.org/advances

1. Introduction

Zinc is the second most essential metal ion for the human body and its biogenic coordination environment plays a number of important roles in a variety of biological processes.[1,2] Like any other main group metal Zn^{II} ions are best known as a structural or catalytic cofactor in a large number of metalloproteins and metalloenzymes. The ligand environment is known to tune the nucleophilicity of the metal bound active site in several hydrolytic enzymes.[3] Understanding of the role of zinc ions in a living system by detecting it in live cells and tissues is an important area of research.[4] To date several Schiff base complexes of zinc(II) are known to show interesting photochromic behavior.[5] The search for new ligand systems responsible for coordination and aggregation of zinc(II) ions has been an active area of research particularly due to the participation of this metal ion in neurobiology.[6] Coordinating primary chelating ligand and small ancillary inorganic anions can control the self-assembly process. Different approaches involving one pot multicomponent synthetic procedure, solvent-based synthesis, hydrothermal and many more are introduced. Solvent free mechanochemical grinding method is an efficient environmentally beneficial approach to reduce environmental contamination.[7] The present work reports the use of a new tetrahydrofuran-based tridentate ligand for zinc coordination induced fluorescence and azido coordination mediated multi-zinc aggregate formation. Azido coordination induced 1D network of zinc(II) is extremely uncommon particularly with Schiff base ligands in comparison to those of manganese(II), nickel(II) and copper(II).[8] Herein a very rare and rather unique 1D zinc(II) coordination polymer is reported using tridentate furan containing Schiff base ligand having triangular Zn_3 motif of two octahedral followed by one tetrahedral zinc(II). Ligand specific coordination plasticity of zinc(II) allows it to show coordination numbers from 3 to 6 and adopts geometries from

Department of Chemistry, Indian Institute of Technology, Kharagpur 721 302, India. E-mail: dray@chem.iitkgp.ernet.in; Fax: +91 3222 82252; Tel: +91 3222 283324

† Electronic supplementary information (ESI) available: Supplementary crystallographic data in CIF format for **1**, **2** and **3**, respectively. CCDC 1006844, 1006845 and 1006846. For ESI and crystallographic data in CIF or other electronic format see DOI: 10.1039/c4ra11352g

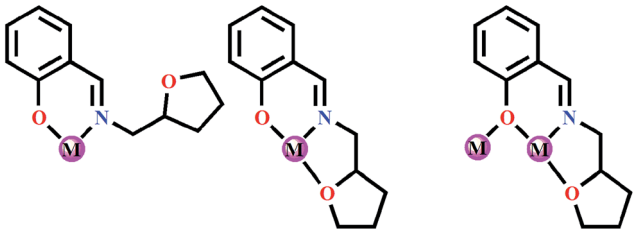

Chart 1 Possible coordination modes of HL.

planar to octahedral with different ligand systems.[9] Known metalloproteins bearing zinc(II) ions quite often show distorted tetrahedral or trigonal bipyramidal geometries.[10] In the absence of any crystal field stabilization, the ligand backbones with rigid, semi-rigid and flexible coordination arms play the deciding role for a particular geometry.[11] Terminal phenoxido group bearing tridentate ligands having pyridine and other terminal ends are known to provide bimetallic and higher order structures.[12] In a particular reaction condition and in support from small ancillary triatomic bridging groups the chosen ligand system can lead to metal ion aggregates.[8] In this work formation of mononuclear, dinuclear and a notable 1D coordination chain from the coordination of (2-hydroxybenzyl-2-tetrahydrofurylmethyl)imine (HL) is achieved with the incorporation of six, five and four coordinated zinc(II) centers by varying the reactants and the reaction conditions. The versatile coordination abilities of furan based tridentate ligand HL (Chart 1) is explored with hydrated zinc perchlorate salt in absence and in presence of triatomic ancillary anions. Depending upon the situation. HL can coordinate as bidentate unit through phenoxido-O and imine-N keeping furfuryl arm as pendent,[13] as tridentate mono-metal centric or can bridge as edge on fashion through phenoxido-O. Participation of furan oxygen in coordination is little known and an interesting observation.[14] Normal tridentate coordination of HL to Zn^{II} provides **1** as mononuclear species. Same reaction in presence of thiocyanato anion yields double-phenoxido-bridged dinuclear complex **2** with pentacoordinated zinc centers. On the other hand, presence of azido anion leads to double-phenoxido and azido bridged complex **3** as a polymeric 1D chain bearing hexacoordinated Zn_2 units flanked by tetrahedral zinc(II) ions in a zigzag arrangement. All three complexes have been synthesized in good yield, and characterized by elemental analysis, FTIR, UV-Vis spectroscopy, and single crystal X-ray diffraction respectively. Moreover their anion dependent aggregation, solvent-free mechanochemical solid state core conversion and photophysical properties were investigated for a systematic study of Zn(II) coordination chemistry involving THF-arm bearing Schiff base ligand.

2. Experimental sections

2.1. Materials

The chemicals used were obtained from the following sources: tetrahydrofurfurylamine from Alfa Aesar, salicylaldehyde from Spectrochem Pvt Ltd, triethylamine and ammonium thiocyanate from S d Fine-Chem Ltd, sodium azide from Merck, India. Zinc(II) perchlorate hexahydrate was prepared by treating zinc carbonate with 1 : 1 conc. $HClO_4$–water mixture and crystallized after concentration on water bath. All other chemicals and solvents were reagent grade materials and were used as received without further purification.

2.2. Synthesis

(2-Hydroxybenzyl-2-tetrahydrofurylmethyl)imine (HL). The ligand HL was prepared *in situ*, following a modified literature procedure,[15] by treating a methanolic solution (10 mL) of tetrahydrofurfuryl amine (0.515 g, 5 mmol) and salicylaldehyde (0.52 g, 5 mmol) under stirring condition at room temperature for 1 h followed by heating at 40 °C for another 45 min (Scheme S1, ESI†). Room temperature solvent evaporation results a light yellow gummy and sticky mass. Yield: 0.81 g (79%). Selected FT-IR bands: (KBr, cm^{-1}; s = strong, vs = very strong, m = medium, br = broad) 3445(br), 2869(m), 1631(vs), 1498(m), 1280(s), 1074(m), 757(s). ^{1}H NMR ($CDCl_3$): δ = 1.66–1.72 (m, 1H), 1.74–1.90 (m, 2H), 1.97–2.10 (m, 1H), 3.60–3.68 (m, 2H, CH_2), 3.69–3.71 (m, 1H, CH_2), 3.73–3.84 (m, 1H, CH_2), 4.10–4.16 (m, 1H, CH), 6.81–6.85 (m, 1H, Ph), 6.92 (d, 1H, J = 8.4 Hz, Ph), 7.21–7.28 (m, 2H, Ph), 8.32 (s, 1H, CH), 13.42 (br, 1H, OH) ppm. ^{13}C NMR ($CDCl_3$): δ = 25.8 (CH_2), 29.1 (CH_2), 63.4 (CH_2), 68.3 (CH), 78.0 (CH_2), 116.9 (CH-Ph), 118.4 (CH-Ph), 118.8 (Cq, Ph), 131.3 (CH-Ph), 132.1 (CH-Ph), 161.2 (Cq, Ph), 166.3 (CH, imine) ppm.

2.3. Complexes

$[H_3O][ZnL_2]ClO_4$ (1). To the methanolic solution (10 mL) of *in situ* generated ligand HL (0.2 g, 1 mmol) solid $Zn(ClO_4)_2\cdot 6H_2O$ (0.19 g 0.5 mmol) was added while stirring at room temperature over a period of *ca.* 15 min. The color of the solution turns yellow upon addition of triethylamine (0.14 mL, 1 mmol) and stirring was continued for further 2 h. After slow evaporation of solvent in air during 5 days, yellow rod like crystals suitable for X-ray diffraction were separated at the bottom of the reaction vessel. One of X-ray diffraction quality crystals was selected and mounted for structure determination. Yield: 0.35 g (59%). Anal. calc. for $C_{24}H_{31}ClN_2O_9Zn$ (592.35 g mol^{-1}): C, 48.66; H, 5.27; N, 4.73. Found: C, 48.83; H, 5.48; N, 4.55. Selected FT-IR bands: (KBr, cm^{-1}; s = strong, vs = very strong, m = medium, br = broad) 3598(br), 1638(vs), 1466(m), 1288(m), 1086(s, br), 758(s), 624(s). Molar conductance, Λ_M: (MeOH solution) 105 S m^2 mol^{-1}. UV-Vis spectra [λ_{max}, nm (ε, L mol^{-1} cm^{-1})]: (MeOH solution) 361 (505), 268 (8270), 236 (17 121).

$[Zn_2(\mu\text{-}L)_2(NCS)_2]$ (2). Method A *via* direct route. To the methanolic solution (10 mL) of $Zn(ClO_4)_2\cdot 6H_2O$ (0.37 g, 1 mmol) was added ligand HL dropwise (0.2 g, 1 mmol) with magnetic stirring. The resulting solution gradually turned to straw yellow upon successive addition of triethylamine (0.14 mL, 1 mmol) and a methanolic solution (5 mL) of ammonium thiocyanate (0.08 g, 1 mmol). After stirring for about 1 h, the reaction mixture was filtered and kept for crystallization. X-ray diffraction quality parallelepiped shaped yellow crystals were

obtained during 5 days. One of these single crystals suitable for X-ray diffraction was mounted for crystal structure determination. Yield: 0.48 g (82%). Anal. Calc. for $C_{26}H_{28}N_4O_4S_2Zn_2$ (655.44 g mol^{-1}): C, 47.64; H, 4.31; N, 8.55. Found: C, 47.61; H, 4.30; N, 8.60. Selected FT-IR bands: (KBr, cm^{-1}; s = strong, vs = very strong, m = medium) 2954(m), 2089(vs), 1633(vs), 1472(m), 1281(s), 1199(m), 905(m), 759(s), 593(m). Molar conductance, Λ_M: (MeOH solution) 30 S m^2 mol^{-1}. UV-Vis spectra [λ_{max}, nm (ε, L mol^{-1} cm^{-1})]: (MeOH solution) 363 (695), 266 (1185), 221 (3119).

*Method B via mechanochemical conversion of **1**.* Quantitative conversion of **1** to **2** was achieved under solvent free condition by thorough mixing and grinding of **1** (0.06 g, 0.1 mmol) with $Zn(ClO_4)_2\cdot 6H_2O$ (0.037 g, 0.1 mmol) and ammonium thiocyanate (0.015 g, 0.2 mmol) in an agate mortar for about 45 min. Addition of water to the grinded paste results a suspension following dissolution of water soluble ammonium thiocyanate. It was filtered followed by careful washing with water–methanol mixture (5 : 1 v/v) to remove un-reacted complex **1** and finally dried under vacuum over P_4O_{10}. Yield: 0.05 g (91%). The yellow powdered product was used for elemental analysis, FT-IR and powder X-ray diffraction analysis (Fig. S2, ESI†). Anal. calc. for $C_{26}H_{28}N_4O_4S_2Zn_2$ (655.44 g mol^{-1}): C, 47.64; H, 4.31; N, 8.55. Found: C, 47.60; H, 4.33; N, 8.51. Selected FT-IR bands: (KBr, cm^{-1}; s = strong, vs = very strong, m = medium) 2957(m), 2087(vs), 1634(vs), 1474(m), 1280(s), 1195(m), 909(m), 761(s), 592(m).

$[Zn_3(\mu\text{-}L)_2(\mu\text{-}N_3)_4]_n$ (3). Method A *via* direct route. The light yellow compound **3** was obtained following method A of complex **2** using NaN_3 (0.13 g, 2.0 mmol) instead of NH_4SCN. Flake type of single crystals suitable for X-ray analysis was obtained from a saturated solution of CH_2Cl_2–MeOH (1 : 10 v/v) after 7 days. One diffraction quality crystal was selected, cleaned with paraffin oil and used for X-ray structure determination. Yield: 0.65 g, (84%). Anal. Calc. for $C_{24}H_{28}N_{14}O_4Zn_3$ (772.77 g mol^{-1}): C, 37.30; H, 3.65; N, 25.38. Found: C, 37.32; H, 3.63; N, 25.35. Selected FT-IR bands: (KBr, cm^{-1}; s = strong, vs = very strong, m = medium, br = broad) 2957(br), 2107(s), 2085(vs), 1645(s), 1550(m), 1294(s), 1198(m), 906(m), 756(m). Molar conductance, Λ_M: (MeOH solution) 18 S m^2 mol^{-1}. UV-Vis spectra [λ_{max}, nm (ε, L mol^{-1} cm^{-1})]: (MeOH solution) 360 (695), 266 (1185), 221 (3119).

*Method B via mechanochemical conversion of **1**.* The complex **3** was also obtained by mechanochemical grinding of **1** (0.06 g, 0.1 mmol) following method B of complex **2**. Here $Zn(ClO_4)_2\cdot 6H_2O$ (0.075 g, 0.2 mmol) and NaN_3 (0.025 g, 0.4 mmol) were mixed and grinded with **1** (0.06 g, 0.1 mmol). A solid mass formed during 30 min of grinding. It was suspended with water then filtered and finally kept under vacuum over P_4O_{10}. The off white fine powder was used for elemental analysis, FT-IR and powder X-ray diffraction analysis (Fig. S2, ESI†). Yield: 0.07 g (89%). Anal. calc. for $C_{24}H_{28}N_{14}O_4Zn_3$ (772.77 g mol^{-1}): C, 37.30; H, 3.65; N, 25.38. Found: C, 37.33; H, 3.61; N, 25.35. Selected FT-IR bands: (KBr, cm^{-1}; s = strong, vs = very strong, m = medium, br = broad) 2951(br), 2109(s), 2083(vs), 1646(s), 1553(m), 1292(s), 1195(m), 908(m), 759(m).

Caution! Although no incidents were recorded in this study, azido complexes of metal ions involving organic ligands are potentially explosive. Only a small amount of material should be prepared, and it should be handled with proper care.

2.4. Physical measurements

The elemental analysis (C, H, N) were performed with a Perkin-Elmer model 240C elemental analyzer. Fourier transform infrared (FT-IR) spectra were recorded on a Perkin-Elmer RX1 spectrometer. Solution electrical conductivity measurements were carried out using a Unitech type U131C digital conductivity meter with a solute concentration of about 10^{-3} M. The powder X-ray diffraction (XRD) measurements were carried out in a PW1710 diffractometer, a Philips, Holland, instrument. The absorption and fluorescence spectra were collected using a Shimadzu (model no. UV-2450) spectrophotometer and a Hitachi (model no. F-7000) spectrofluorimeter respectively. For steady-state measurements, all the samples were excited at 380 nm to collect the emission spectra. For time-resolved measurements, we used a time correlated single-photon-counting (TCSPC) instrument from IBH (U.K.). The samples were excited at 450 nm using a picosecond laser diode (IBH, Nanoled), and the signals were collected at the magic angle (54.7°) using a Hamamatsu microchannel plate photomultiplier tube (3809U). The same setup was used for anisotropy measurements. The instrument response function of our setup is ~90 ps. The excellence of the fit was judged by the χ^2 criterion. In multi-exponential decay at least two distinct lifetimes are present. Average fluorescence lifetime (τ_{av}) for bi-exponential decay curve was obtained from the decay time constants (τ) and pre-exponential factors (a) using eqn (1) where τ_1 and τ_2 are the two relaxation time constants with normalized pre-exponential factors a_1 and a_2 respectively

$$\tau_{av} = \tau_1 a_1 + \tau_2 a_2 \quad (1)$$

Fluorescence quantum yields (Φ) of all the compounds were determined at room temperature from methanol solution by comparing the corrected spectrum with that of anthracene (Φ = 0.27) in ethanol[16] as the secondary standard using eqn (2).

$$\frac{\Phi_S}{\Phi_R} = \frac{A_S}{A_R} \times \frac{(Abs)_R}{(Abs)_S} \times \frac{{n_S}^2}{{n_R}^2} \quad (2)$$

where A is the integrated area under the emission spectral curve, Abs denotes absorbance at the wavelength of exciting light, η is the refractive index of the medium, Φ is the fluorescence quantum yield, and the subscripts S and R stand in the recognition of the respective parameters of studied sample and reference, respectively.

2.5. Crystal data collection and refinement

The X-ray diffraction data of the complex **1**, **2** and **3** were collected on a Bruker APEX-II CCD X-ray diffractometer using single crystals that uses graphite-monochromated Mo-K_α radiation (λ = 0.71073 Å) by ω-scan method at 298 K. Information concerning X-ray data collection and structure refinement of the

Table 1 Crystallographic data and refinement parameters of complexes **1**, **2**, and **3**

Complex	**1**	**2**	**3**
Formula	$C_{24}H_{28}ClN_2O_9Zn$	$C_{26}H_{28}N_4O_4S_2Zn_2$	$(C_{24}H_{28}N_{14}O_4Zn_3)_n$
M/g mol^{-1}	589.32	655.44	772.77
Space group	$C2/c$	$P21/c$	$P2/c$
Cryst syst	Monoclinic	Monoclinic	Monoclinic
a/Å	23.365(3)	6.8404(8)	11.6671(8)
b/Å	12.7460(18)	21.759(2)	10.8103(7)
c/Å	17.904(2)	9.8058(11)	12.2636(9)
β/deg	101.513(4)	106.686(3)	103.876(2)
V/Å^3	5224.7(12)	1398.9(3)	1501.61(18)
T/K	293	293	293
Z	8	2	2
D_c/g cm^{-3}	1.498	1.556	1.709
F(000)	2440	672	784
μ(Mo-Kα)/cm^{-1}	10.97	19.03	24.34
Cryst dimens (mm^3)	0.31 × 0.22 × 0.13	0.29 × 0.21 × 0.13	0.33 × 0.22 × 0.15
No. of reflns collected	32 409	15 239	14 465
No. of unique reflns	5476	2628	2614
No. of params	334	172	204
R_1; wR_2 ($I > 2\sigma(I)$)	0.0584; 0.1555	0.0410; 0.0954	0.0579; 0.1278
R(int)	0.0564	0.0184	0.0372
GOF (F^2)	1.037	1.138	1.020
CCDC nO.	1006844	1006845	1006846

compound is summarized in Table 1. The SMART software was used for data acquisition. Data integration and reduction were performed with SAINT and XPREP software.[17] Structures were solved by direct methods using SHELXS-97 [18] and refined with full-matrix least squares on F^2 using the SHELXL-97 [19] program package. All non-hydrogen atoms were refined anisotropically. Multiscan absorption corrections were applied to the data using the program SADABS.[20] The locations of the heaviest atom (Zn) and the other atoms O, N, S, Cl, and C were subsequently determined from the difference Fourier maps. The H atoms were introduced in calculated positions and refined with fixed geometry with respect to their carrier atoms. A summary of the crystal data and relevant refinement parameters are given in Table 1.

3. Results and discussion

3.1 Synthetic considerations

The ligand HL was prepared by a single step 1 : 1 condensation of tetrahydrofurfurylamine and salicylaldehyde in methanol (Scheme S1, ESI†). It was characterized by FT-IR and NMR spectral measurements. The characteristic vibration of imine bond appeared at 1631 cm^{-1}. In ^{1}H NMR spectrum of the ligand in $CDCl_3$, the characteristic imine proton appears at 8.32 ppm, the broad phenolic OH peak at 13.42 ppm whereas the hydrogen of the aromatic phenol and the tetrahydrofurfuryl rings are at 6.81–7.28 and 1.66–4.16 ppm, respectively. ^{13}C NMR spectrum records peak at 166.3 ppm for imine carbon. The potential metal binding abilities of HL (Chart 1) was next investigated using hydrated zinc(II) perchlorate salt in presence of triethylamine and exogenous bridging units like azido and thiocyanato ions as summarized in Scheme 1.

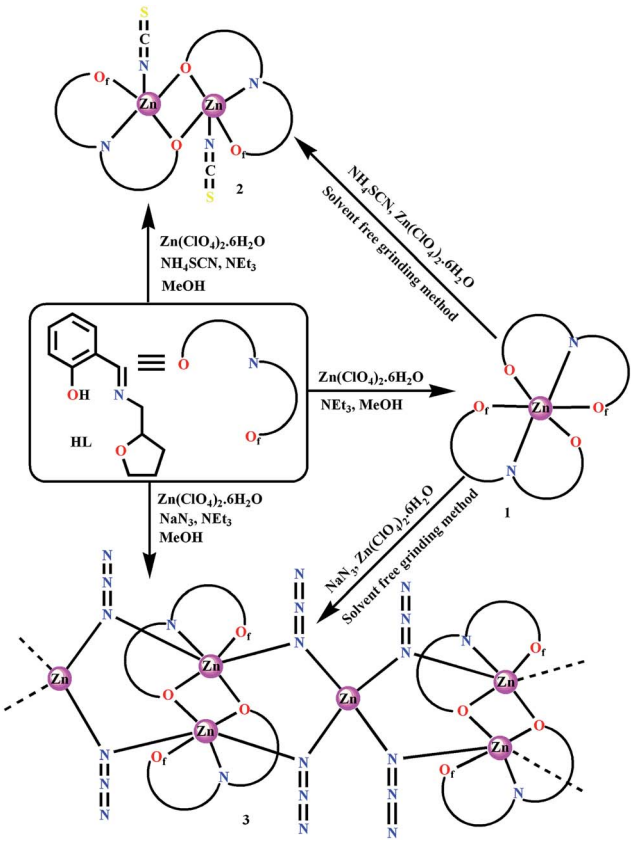

Scheme 1 Summary of the possible synthetic routes for the complexes **1–3**.

When $Zn(ClO_4)_2\cdot 6H_2O$ was treated with HL in 1 : 2 metal–ligand ratio in MeOH and NEt_3 base, **1** results as yellow crystal directly from the reaction mixture in moderate yield. The preparation of **1** is summarized in eqn (3).

$$2HL + Zn(ClO_4)_2\cdot 6H_2O + NEt_3 \rightarrow [H_3O][ZnL_2]ClO_4 + NHEt_3ClO_4 + 5H_2O \quad (3)$$

Using a similar approach, two other reactions have been carried out in the presence of thiocyanato and azido anions. In both the cases, bis-chelation by two tridenate ligands is prevented due to the simultaneous coordination of these externally added anions. Yellow complexes **2** and **3** (Scheme 1) are directly synthesized in ~80% yield from MeOH solution under aerobic conditions at room temperature by stirring the reaction mixture of HL, $Zn(ClO_4)_2\cdot 6H_2O$, NEt_3 and NH_4SCN or NaN_3 in 1 : 1 : 1 : 1 or 1 : 1.5 : 1 : 2 molar ratio for 1 h respectively. The synthesis of **2** and **3** are summarized in eqn (4) and (5) respectively

$$2HL + 2Zn(ClO_4)_2\cdot 6H_2O + 2NEt_3 + 2NH_4SCN \rightarrow [Zn_2(\mu\text{-}L)_2(NCS)_2] + 2NHEt_3ClO_4 + 2NH_4ClO_4 + 12H_2O \quad (4)$$

$$2nHL + 3nZn(ClO_4)_2\cdot 6H_2O + 2nNEt_3 + 4nNaN_3 \rightarrow [Zn_3(\mu\text{-}L)_2(\mu\text{-}N_3)_4]_n + 2nNHEt_3ClO_4 + 4nNaClO_4 + 18nH_2O \quad (5)$$

The elemental analysis and molar conductivity data confirm the respective formula for these compounds. Reactions with an excess of thiocyanato or azido anions did not lead to the substitution of the terminal tetrahydrofuran oxygen coordination to the zinc ions in **2** and **3**, indicating a reasonably strong affinity and stability of the tetrahydrofuran binding in these systems. During these synthesis we have not encountered with any kind of SCN^- or N_3^- coordination induced partial extrusion of anionic zinc based species like $Cu_2(NCS)_6^{2-}$ or $Cu(N_3)_4^{2-}$.[21]

A fundamentally different route of initiating and accelerating these reactions have been explored through use of force in the form of mechanical grinding in solid state for the transformation of **1** to **2** and **1** to **3**. Solid state transformation from one species to another is a topic of contemporary relevance especially in solvent free solid-state synthesis. Thorough mixing and grinding of basic complexing unit **1**, $Zn(ClO_4)_2\cdot 6H_2O$ and exogenous bridging units NaN_3 and NH_4SCN in 1 : 1 : 2 and 1 : 2 : 4 molar ratio proceed through the formation of paste followed by solidification. Initially it is expected that 1 : 1 reaction between **1** and $Zn(ClO_4)_2\cdot 6H_2O$ produces an intermediate species, [Zn(L)(ClO_4)] where mononegative tridentate ligand and perchlorido ion simultaneously coordinated to the Zn^{II} center leaving behind vacant sites around the Zn^{II} ion. Addition of thiocyanato anion replaces perchlorido anion from the coordination environment because of its stronger coordinating ability. The reaction involved for the synthesis of **2** *via* mechanochemical grinding is summarized in eqn (6).

$$[H_3O][ZnL_2]ClO_4 + Zn(ClO_4)_2\cdot 6H_2O + 2NH_4SCN \rightarrow [Zn_2(\mu\text{-}L)_2(NCS)_2] + 2NH_4ClO_4 + HClO_4 + 7H_2O \quad (6)$$

Compound **3** on the other hand, is formed *via* azido coordination induced trapping of Zn^{II} ions by ligand bound $[Zn_2L_2]$ fragments. A rare 1D chain is obtained both by solvent based multicomponent approach and mechanochemical route containing Zn^{II} : L in 3 : 2 ratio in the basic unit. The reaction involved during mechanochemical transformation is summarized in eqn (7).

$$[H_3O][ZnL_2]ClO_4 + 2nZn(ClO_4)_2\cdot 6H_2O + 4nNaN_3 \rightarrow [Zn_3(\mu\text{-}L)_2(\mu\text{-}N_3)_4]_n + 4nNaClO_4 + HClO_4 + (12n + 1)H_2O \quad (7)$$

Thus the use of exogenous units not only inhibits the bis-chelation around Zn^{II} but also promotes the ligand to act as bridging unit. Furthermore solvent free mechanochemical grinding method not only develops new topologies and metal–ligand aggregation but also shows the solid state core conversion and ligand exchange from octahedral to square pyramidal in **1** to **2** and octahedral to 1D coordination network containing two octahedral units followed by one tetrahedral in **1** to **3**. These transformations were confirmed by comparing the solubility differences, FTIR spectra (Fig. S1, ESI†) and unit cell parameters of single crystals grown from powder samples. The powder X-ray diffraction (PXRD) patterns (Fig. S2, ESI†) of complexes **1–3** are consistent with those of simulated ones (Fig. S3, ESI†) obtained based on the structures derived from the single crystal X-ray measurements, suggesting the phase change during the core conversions within the complexes. Furthermore it concludes the bulk materials are consistent with same chemical constituents that resembles with the crystal structures.

3.2. IR spectroscopy

The characteristic band of $\tilde{\nu}_{C=N}$ stretching vibration of ligand HL appears at 1631 cm^{-1} and broad band around 3435 cm^{-1} is due to –OH stretching. The sharp peaks in the spectra of **1–3**, at 1633–1645 cm^{-1} are due to Zn^{II}-bound –C=N stretching vibrations whereas peaks at 1281–1294 cm^{-1} are due to $\tilde{\nu}_{C-O}$ vibrations of the coordinated L^- ligands.[22] In complex **1**, a sharp band at 3597 cm^{-1} is observed due to hydrogen bonded –OH vibrations from water of crystallization, whereas strong and sharp peaks at 1086 cm^{-1} and 624 cm^{-1} are for IR active asymmetric stretching (ν_3) and asymmetric Cl–O bending (ν_4) vibrations of intimately hydrogen bonded (O···O distance 2.622–2.739 Å, *vide supra*) ClO_4^- unit present in the crystal lattice. The characteristic band at 2089 cm^{-1} of $\tilde{\nu}_{C-N}$ stretching mode in **2** is due to terminally Zn^{II}-bound SCN^- group. The $\tilde{\nu}_{as(N-N-N)}$ asymmetric stretching vibrations of metal bound $\mu_{1,1}$-N_3^- groups at 2085 cm^{-1} along with a kink around at 2107 cm^{-1} appear for **3**.

3.3. X-ray crystal structural descriptions

Yellow crystals of **1** obtained from a saturated solution of MeOH, crystallizes in monoclinic *C*2/*c* space group. A perspective view of **1** is presented in Fig. 1 and selected bond distances and angles around the metal center are listed in Table 2. The structural analysis reveals that **1** has a bis-chelated mononuclear structure containing a hexacoordinated Zn^{II} ion having

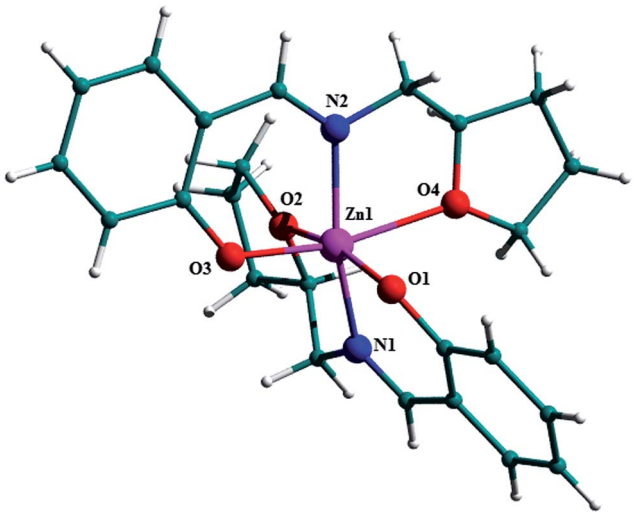

Fig. 1 Pov-Ray view of **1** with partial atom numbering scheme. Color code. C, teal; H, white, N, blue; O, red; Zn, pink. ClO_4^- and H_3O^+ ions are omitted for clarity.

two tridentate L^- ligands in *meridional* binding mode. A distorted N_2O_4 octahedral environment around the Zn^{II} center is found from almost planar ONO^- coordination of two L^- units.

The individual L^- units remain perpendicular (89.2°) to each other. The neutral tetrahydrofuran oxygen coordination provides longer Zn–O bonds in 2.235–2.306 Å compared to mono-metal centric phenoxido oxygen donors (2.052–2.071 Å). The shortest Zn–N bond distances are from imine nitrogen coordination of 2.026–2.035 Å. The six-membered bite (88.5–90°) containing the phenoxido donor is greater than the tetrahydrofuran bearing five-membered chelate ring (77.3–77.4°). The five- and six-members chelate rings form inter-planar angles of 4.9–15.4° range.

In **1** the counter ions ClO_4^- and H_3O^+ are stabilized by intricate hydrogen bonding interactions. The H-atoms could not be located from the difference Fourier map and Q peaks after refinement steps. The hydrogen bonding parameters are listed in Table 3. It is clear from the Fig. 2 that two H_3O^+ and two ClO_4^- ions associate six monomeric ZnL_2 units through three types of hydrogen bonding interactions; C–H···O, Cl–O···H and O–H···O respectively. There are six C–H···O interactions of 2.551–2.717 Å range with C–H fragments from ligands backbone (H5, H7, H10A, H11A, H12A and H19), two with each water oxygen (O9W) and four with two oxygen atoms (O6 and O8) of each perchlorido anion. Through two Cl–O···H_W and two O–H_W···O interactions both perchlorido oxygen (O7) and H_3O^+ ion form an eight membered cyclic ring (Fig. S4, ESI†). The O···O and C···O distances are 2.622–2.739 Å and 3.489–3.606 Å and the C–H···O angles are 132.52–165.43° respectively.

Complex **2** as shown in Fig. 3 crystallizes in monoclinic *P*21/*c* space group directly from the methanol reaction mixture. The selected bond distances and angles are given in Table 2. It is a centrosymmetric double phenoxido bridging dinuclear zinc(II), with the inversion center located at the midpoint of Zn_2O_2 diamond core. Here two L^- ligands through edge on bridging

Table 2 Selected bond distances (Å) and bond angles (°) in **1**, **2** and **3**

Bond distances (Å)			
Complex 1			
Zn1–N2	2.026(4)	Zn1–O1	2.071(4)
Zn1–N1	2.035(4)	Zn1–O2	2.239(4)
Zn1–O3	2.052(3)	Zn1–O4	2.305(4)
Complex 2			
Zn1–N2	1.958(3)	Zn1–O2	2.261(3)
Zn1–O1	1.989(2)	Zn1···Zn1	3.1011(8)
Zn1–N1	2.025(3)	Zn1–O1	2.071(2)
Complex 3			
Zn1–O1	2.049(4)	Zn1–Zn1*	3.1855(14)
Zn1–N1	2.120(6)	Zn2–N5	2.037(5)
Zn1–N2	2.131(5)	Zn1–O2	2.345(5)
Zn1–O1	2.098(4)	Zn2–N2	1.989(5)
Zn1–N5	2.120(5)		
Bond angles (°)			
Complex 1			
N2–Zn1–N1	160.62(17)	N1–Zn1–O1	88.55(16)
N2–Zn1–O3	89.96(15)	O3–Zn1–O1	89.66(13)
N1–Zn1–O3	106.57(16)	N2–Zn1–O2	91.78(17)
N2–Zn1–O1	101.89(16)	N1–Zn1–O2	77.21(17)
O3–Zn1–O2	94.40(16)	O3–Zn1–O4	166.72(14)
O1–Zn1–O2	165.76(14)	O1–Zn1–O4	89.77(16)
N2–Zn1–O4	77.19(17)	O2–Zn1–O4	89.33(18)
N1–Zn1–O4	86.68(17)		
Complex 2			
N2–Zn1–O1	111.67(13)	N1–Zn1–O1	88.53(11)
N2–Zn1–N1	120.99(14)	N2–Zn1–O2	90.65(12)
O1–Zn1–N1	127.17(12)	O1–Zn1–O2	98.92(10)
N2–Zn1–O1	106.51(13)	N1–Zn1–O2	77.41(10)
O1–Zn1–O1	80.40(10)	O1–Zn1–O2	161.89(10)
Complex 3			
O1–Zn1–O1	79.65(17)	O1–Zn1–O2	118.56(17)
O1–Zn1–N5	98.01(18)	N5–Zn1–O2	88.91(18)
O1–Zn1–N5	85.22(18)	N1–Zn1–O2	74.5(2)
O1–Zn1–N1	87.5(2)	N2–Zn1–O2	85.40(18)
O1–Zn1–N1	166.8(2)	N2–Zn2–N2	125.4(3)
N5–Zn1–N1	93.7(2)	N2–Zn2–N5	103.2(2)
O1–Zn1–N2	89.81(17)	N2–Zn2–N5	109.5(2)
O1–Zn1–N2	90.64(18)	N1–Zn1–N2	92.3(2)
N5–Zn1–N2	170.3(2)	O1–Zn1–O2	161.16(17)

Table 3 Hydrogen bonding parameters for the crystal structure of complex **1**

Interactions	D–H (Å)	D···A (Å)	H···A (Å)	D–H···A (°)
C–H10A···O_{9W}	0.970	3.489	2.557	161.39
C–H10A···O_{9W}	0.970	3.606	2.717	152.51
C–H11A···O_8	0.971	3.607	2.677	160.47
C–H7···O_8	0.929	3.330	2.631	132.52
C–H5···O_6	0.930	3.357	2.551	145.28
C–H19···O_6	0.929	3.622	2.716	165.43

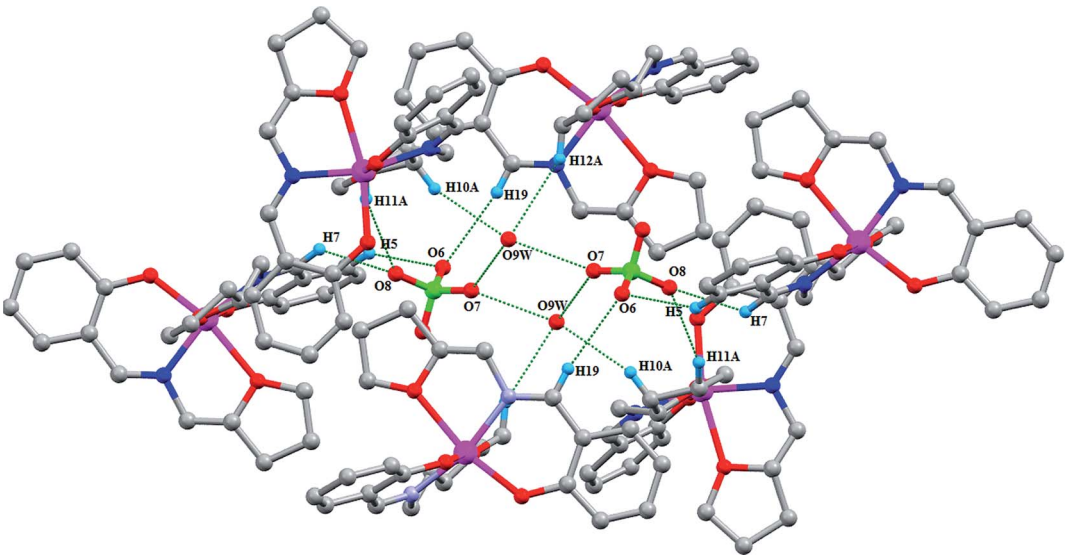

Fig. 2 Hydrogen bonding interactions of lattice ClO_4^- and H_3O^+ ions and C–H···O interactions in complex **1**. Color code: C, grey; H, aqua; N, blue; O, red; Cl, green; Zn, pink. Only participated hydrogen atoms are shown.

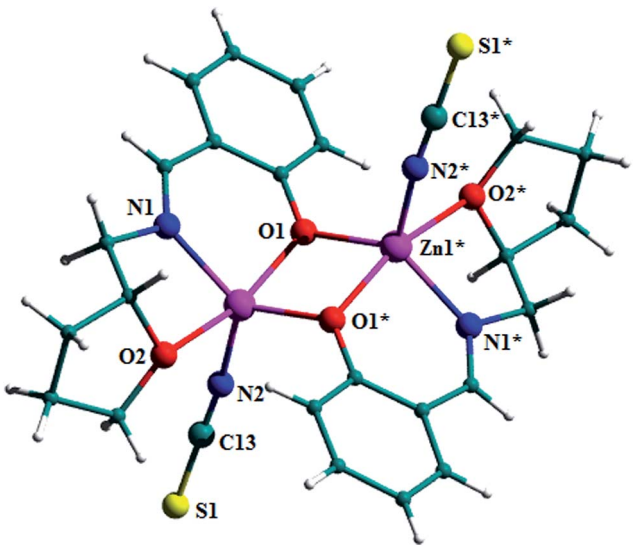

Fig. 3 Pov-Ray view of **2** with partial atom numbering scheme. Color code: C, teal; H, white, N, blue; O, red; S, yellow; Zn, pink. Symmetry code: $-x$, $-y$, $-z$.

fashion provide distorted square planar coordination around each Zn^{II} ion with imine-N, tetrahydrofurfuryl-O and μ-phenoxido oxygen. To this coordinatively unsaturated system, through terminal coordination, isothiocyanato anions occupy apical position to satisfy distorted square pyramidal geometry. The Zn–O distance (2.261 Å) for tetrahydrofurfuryl-O coordination is significantly longer as compared to the Zn–O distances from phenoxido bridges (1.989–2.071 Å). The Zn–N distance is longer for imine coordination (2.025 Å) than for isothiocyanato binding (1.958 Å). The Zn1···Zn1* separation (3.101 Å) is shorter by 0.1 Å compared to the range of previously reported doubly bridged dizinc complexes.[23] The six-membered bite angle (88.5°) is greater than the five-membered one (77.4°). The inter-planar angle between the five- and six-members chelate rings is 12.4°. The degree of distortion around pentacoordinate Zn^{II} environments (Zn1 and Zn1* respectively) is calculated with Addison parameter, $\tau_5 = 0.59$ ($\tau = |\beta - \alpha|/60°$ where β and α are the two largest angles around the central atom. $\tau_5 = 0$ for a perfect square pyramidal and 1 for a perfect trigonal bipyramidal geometry).[24] In the present case the distortion is 59% and hence the geometry of Zn^{II} ion in **2** can be best described as an intermediate between distorted square pyramid and trigonal-bipyramid. Both the Zn^{II} centers are elevated from the mean square plane in opposite direction by 0.601 Å. The core structure consists of two distorted square pyramidal ZnN_2O_3 fragments connecting through a common O,O-edge from bridging phenoxido oxygen atoms (Fig. S5, ESI†).

A perspective view of the rare and novel 1D coordination chain of **3** which crystallizes in monoclinic *P*2/*c* space group is shown in Fig. 4 and selected bond distances and angles are given in Table 2. The repeating Zn_3 asymmetric unit contains two partially developed double phenoxido bridged dinuclear ligand bound Zn_2L_2 units and azido bound $Zn(N_3)_4^{2-}$ unit with chemical formula $[Zn_3(\mu\text{-}L)_2(\mu\text{-}N_3)_4]$ (Fig. S6, ESI†). Both these two units are linterlinked through $\mu_{1,1}$-bridging azido N atoms (N2 and N5*). Among three Zn^{2+} ions in basic Zn_3 motif, two Zn^{II} centers (Zn1 and Zn1*) are in octahedral N_3O_3 coordination environments whereas the third Zn^{II} ion (Zn2) resides in distorted tetrahedral N_4 site. In ZnN_4 environment the tetracoordinate index $\tau_4 = 0.89$ can be best described as tetrahedral geometry [$\tau_4 = \{360 - (\alpha + \beta)\}/141°$, where α and β are two largest angles in the four coordinate geometry].[25]

The distorted octahedral environments around Zn1 and Zn1* can be demonstrated from the deviation of *cis* angles (74.5–98°) and *trans* angles (161.2–166.8°) from the ideal values. Ligand bound Zn_2L_2 unit with an inversion center forms the Zn_2O_2 diamond core with Zn···Zn separation of 3.186 Å whereas all azido bound Zn2 show Zn···Zn separations of 3.484–3.556 Å

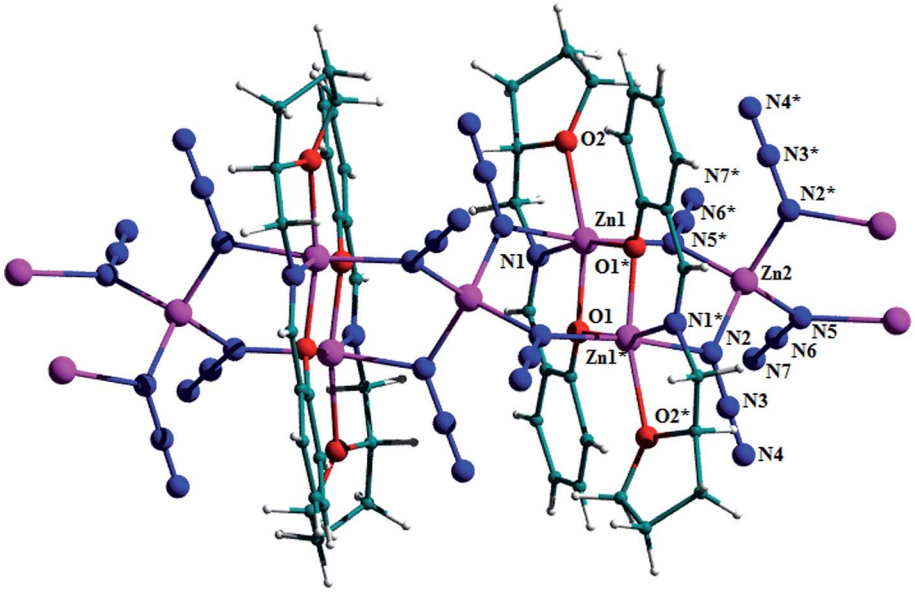

Fig. 4 Pov-Ray view of the 1D zigzag chain (**3**) with partial atom numbering scheme. Color code: C, teal; H, white, N, blue; O, red; Zn, pink. Symmetry code: $-x, -y, -z$.

from L^- bound Zn^{II} centers (Zn1 and Zn1*). Two *apical* N atoms coordination from $\mu_{1,1}$-N_3^- binding complete the octahedral arrangement. The third Zn^{II} ion is tetra-coordinated by four bridging azido groups in a slightly distorted tetrahedral environment. The tetrahedral angles are in 103.2–109.5° around Zn2. In this trinuclear unit the angular Zn1–Zn2–Zn1* disposition makes angles of 64.0° whereas in zigzag arrangement of repeating Zn_3 units make angles of 138.4–161.5°. The unsymmetrical azido bridge Zn–N distances are 1.99 and 2.04 Å respectively whereas Zn–N distance from coordinated imine N falls in between at 2.12 Å. The core structure of **3** consists of four vertex shared octahedral ligand bound ZnN_3O_3 units around the central tetrahedral ligand free ZnN_4 unit and the assembly is repeated as 1D chain (Fig. S7, ESI†).

3.4. Steady-state absorption and emission spectra

The coordination driven change in ground state electronic absorption behavior in MeOH of complexes **1–3** are shown in Fig. 5. The zinc complexes are known to record only the charge transfer transitions as no d–d transitions are expected for d^{10} Zn^{2+} ion.[26] The ligand HL exhibits four primary absorption bands in the UV-visible region at 215, 254, 316 and 398 nm respectively (Table 4). These bands are assigned to the n → π* and π → π* transitions from the Schiff base ligand (*i.e.*, phenolate and the ligand frame-work). The maximum absorption intensity centered at 398 nm due to intraligand n → π* trantion is blue shifted to about 360 nm in complexes **1–3**. The bands at 220, 255 and 320 nm for **1** are possibly due to the π → π* transitions centered mainly on the azomethine chromophore (imine π → π*). The 320 nm band is shifted to the lower wavelength region at 270 nm during zinc(II) coordination in **1**. For **2** and **3** these bands appear very close to those obtained for **1**.

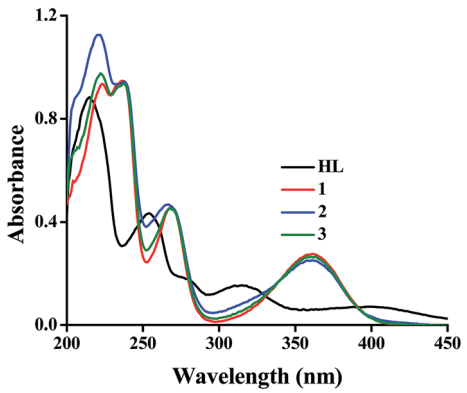

Fig. 5 Experimental UV-Vis absorption spectra of HL and complexes **1–3** (10 μM neat MeOH solution).

Table 4 Absorption and emission parameters,[a] and fluorescence quantum yields[b] of HL and **1–3**

System	λ_{max} (nm) [ε (M^{-1} cm^{-1})]	λ_{em} (nm)	Φ_f
HL	398 (733), 316 (1529), 254 (4336), 215 (8817)	446	0.032
1	361 (2778), 268 (4541), 236 (9755), 223 (9327)	452	0.078
2	360 (2547), 266 (4639), 237 (9460), 221 (11235)	448	0.32
3	360 (2652), 268 (4500), 238 (9371), 221 (3119)	447	0.13

[a] Excitation wavelength is 380 nm. [b] The fluorescence quantum efficiency was determined by using anthracene as reference (Φ_R = 0.27).[16]

Emission properties of HL and three metal complexes were examined in MeOH solution at room temperature (Fig. 6). The observed emission behavior is solely due to the intraligand

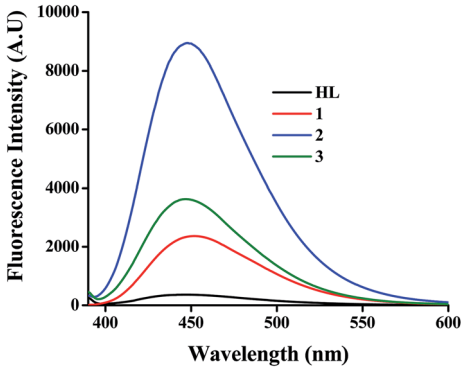

Fig. 6 Fluorescence emission spectra of ligand (10 μM) and metal complexes (10 μM) in neat MeOH solutions.

$\pi \rightarrow \pi^*$ fluorescence since Zn^{II} ion with stable d^{10} configuration is spectroscopically and magnetically inert.[27] The HL molecules form a monomeric ground state with a low quantum yield (Table 4). The enhancement of fluorescence intensities and hence quantum yields in complexes **1–3** is mainly due to different metal–ligand aggregation, in absence and presence of anions, and the nature of the emitting species. The emission intensities of HL shows specific Zn^{II}-binding induced emission characteristics. The emission band of HL is very close to the metal complexes **1–3**.[1] For **1** the fluorescence quantum yield (Φ_f) is increased about 2.5 fold in comparison to free HL whereas the same for **2** and **3** are 4 and 10 fold respectively. This coordination driven enhancement of fluorescence intensity is explainable in terms of attainment of more rigidity upon complexation.[28]

The emission properties of HL in presence of free Zn^{2+} ion were examined in MeOH solution at room temperature (Fig. 7) to identify the change in fluorescence behavior of the ligand during complexation and aggregation. The emission spectrum of 10 μM HL records emission maximum at 446 nm when the solution is excited at 380 nm. The emission intensities of the tridentate zinc chelator HL was measured in the presence of various amounts of $Zn(ClO_4)_2 \cdot 6H_2O$ (0–10 μM). The system shows definite coordination induced enhancement of emission behavior. The emission is maintained at 452 nm upto addition of 1 equiv. of Zn^{2+} leading to the formation of hitherto unknown complex $[Zn(L)(ClO_4)]$ in solution which is different from that of solid state compound **1**. The emission band of the free ligand is almost at the same wavelength as observed during metal–ligand titration, indicating emission takes place from the same excited state. In the absence of metal ions the fluorescence of the ligand is possibly quenched by the occurrence of a photoinduced electron transfer (PET) process due to the presence of lone pair of electrons of the donor atoms in the ligand.[29] Such a PET process is prevented by the complexation of HL with metal ions, thus the fluorescence intensity may be greatly enhanced by the coordination of Zn^{II}. The chelation of the ligand to Zn^{II} increases the rigidity of the ligand and thus reduces the loss of energy by thermal vibrational decay.[30]

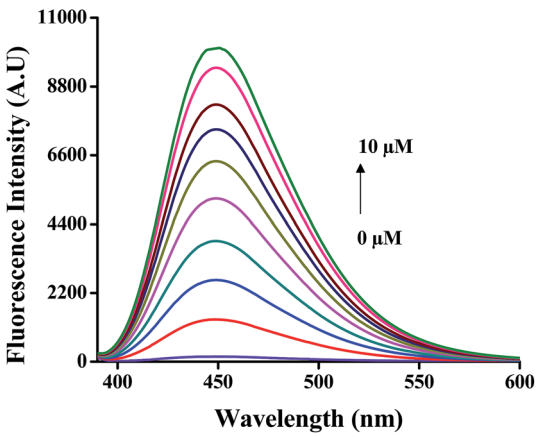

Fig. 7 Emission spectra of HL (10 μM) in presence of 0, 1, 2, 3, 4, 5, 6, 7, 8, 10 μM of free Zn^{2+} ions in neat MeOH at room temperature (excitation 380 nm, emission 449 nm).

Anion dependent fluorescence responses were investigated using **1** as fluorescent probe. Spectrofluometric titration with addition of various amount of NH_4SCN (Fig. 8, left) and NaN_3 (Fig. 8, right) in two separate experiments shows coordination induced quenching of fluorescence intensities up to the addition of 1 equiv. of exogenous anions. The 1 : 1 composition of **1** and exogenous anions forms an hitherto unknown complex $[Zn(L)(X)]$ (where $X = N_3^-$ and SCN^-) which could not be isolated. On excitation at the maximum absorption of **1** (λ_{max} of 360 nm) the emission maximum centered at 450 nm is reproduced which is exactly the same as that obtained during metal–ligand titration. From emission spectra, it is clear that the quenching of emission intensities as compared to **1** is more prominent for **2** than that of **3**. This observation clearly points to the fact that fluorescent emissions are very much sensitive to anion replacement and can be diagnosed for the thiocyanato and azido anions following quenching of emission intensities.

3.5. Time-resolved emission studies

Time-resolved fluorescence (TRF) spectroscopy is known to be a valuable tool for imaging cellular components.[31] Measurements of TRF decay profiles of HL ligand and its Zn^{II} complexes can differentiate between different populations of fluorescence emitting fluorophores with varying lifetimes, whereas steady-state fluorescence measurements identify unresolved contributions of individual components to the overall fluorescence.[32] Thus time resolved fluorescence measurement is most suitable to extract the lifetimes of ligand and the complexes in the excited state. In most cases the fluorescence from these were overlapping but using TRF measurements distinct fluorescence lifetime can be extracted. Lifetime of an excited ligand or complex molecule is the time taken for an ensemble of such molecules to decay to $1/e$ (36.8%) of their initial excited state population. The fluorescence lifetime (τ_{av}) thus refers to the average time a molecule stays in its excited state before emitting a photon. Time-resolved fluorescence emissions of **1–3** along with the free ligand HL were recorded in MeOH solvent at an excitation wavelength of 375 nm and spectra were monitored at the emission wavelength of 450 nm. A comparative decay profile

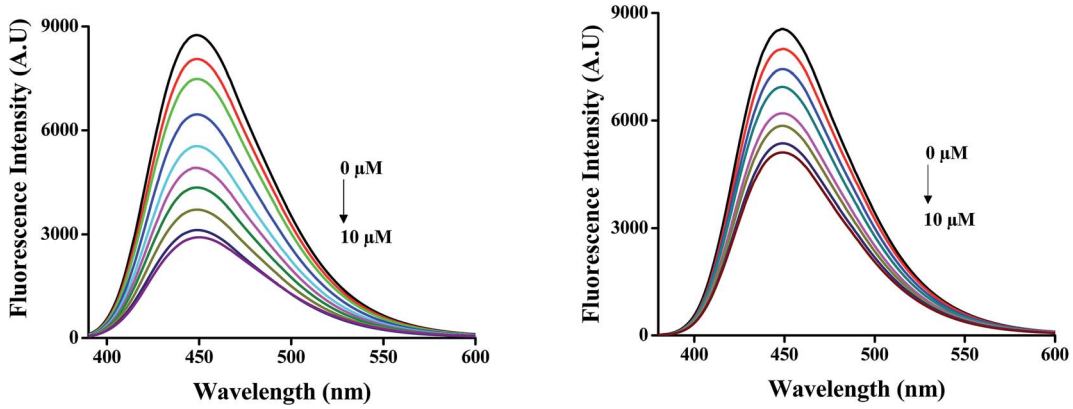

Fig. 8 Emission spectra of **1** (10 μM) in presence of SCN^- (0, 1, 2, 3, 4, 5, 6, 7, 8, and 10 μM) (left) and N_3^- (0, 1, 2, 3, 4, 5, 7, and 10 μM) (right) ions in neat MeOH at room temperature (excitation 380 nm, emission 449 nm).

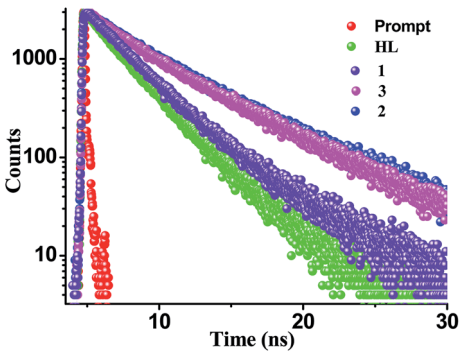

Fig. 9 The comparative decay profile for HL and complexes **1–3**.

is depicted in Fig. 9 and the corresponding lifetime values (τ's) and amplitudes (a's) were obtained using eqn (1) (in Physical Measurements). The fluorescence lifetime is not affected by the concentration of the fluorophores, static quenching effects, or the brightness of the light source. In contrast, dynamic quenching, resonance energy transfer, and temperature have a strong impact on the fluorescence decay. Thus, the fluorescence lifetime is a preferred parameter in fluorescence sensing and imaging. The biexponential fitting of the decay processes provide the parameters which are given in Table 5.

The average lifetime (τ_{av}) of HL is measured at 2.50 ns with two relaxation time constants (τ's) of 1.78 ns (55%) and 3.37 ns (45%) having pre-exponential factors of 0.55 and 0.45. In complex **1** and **2** these τ_{av}'s are higher at 4.56 and 4.80 ns and with τ's of 2.30 and 2.47 ns (38.8% each) and 6.00 and 6.27 ns (61.2% each) respectively, whereas in complex **3** the τ_{av} is very close to the value for HL at 2.97 ns but the τ's are significantly different at 2.46 ns (80.2%) and 5.01 ns (19.8%). These values clearly indicate the different excited state lifetime for all these species. These results can be compared in terms of the environment of the tryptophan residue in the proteins.[33] The lifetime of tryptophan residues in proteins range from ~0.1 ns to ~8 ns. For a bi-exponential fit the lifetime distributions of the two conformations spread in adjacent lifetime intervals. The longer lived conformation extends in the 6 ns to 9 ns range and shorter lived conformation extends in the 2 ns to 5 ns range.[34]

Table 5 Photophysical parameters of ligand and metal complexes at an excitation wavelength of 450 nm

Compound	τ_1, ns (a_1)	τ_2, ns (a_2)	τ_{av}, ns	χ^2
HL	1.78 (0.55)	3.37 (0.45)	2.50	1.08
1	2.30 (0.388)	6.00 (0.612)	4.56	0.96
2	2.47 (0.388)	6.27 (0.612)	4.80	0.92
3	2.46 (0.802)	5.01 (0.198)	2.97	0.95

4. Concluding remarks

We have investigated the coordination and photophysical response of tetrahydrofuran bearing Schiff base HL with Zn^{II} in absence and presence of thiocyanato and azido ions. Mechanochemical solid state core conversion through ligand exchange is applied for the synthesis of **2** and **3** using **1** as basic complexing agent. Here mononuclear octahedral core in **1** is converted into edge sharing square pyramidal units in **2** and vertex sharing two octahedral fragments followed by one tetrahedral core in repeated fashion in **3**. In solvent based synthesis a single L^- bound zinc(II) plays the crucial role as basic template unit for the subsequent formation of three complexes from competitive coordination of the inorganic anions. We have successfully achieved the synthesis of three different coordination geometries from the same tridentate ligand with very uncommon coordination of tetrahydrofuran oxygen. The photophysical characterizations showed that the chelation induced emission behaviors of complexes **1–3** and significant increase in fluorescence quantum yield in comparison to free HL. Spectrofluometric titrations of HL with Zn^{II} showed coordination induced fluorescence enhancement whereas **1** showed quenching behaviors in presence of externally added N_3^- and SCN^- anions. In comparison to the ligand itself, the complexes record different excited state lifetime which are comparable to that of the tryptophan residue in different protein part.

Acknowledgements

HM is thankful to the Council of Scientific and Industrial Research, New Delhi for the financial support. We are thankful to Prof. Nilmoni Sarkar for providing the instrumental facility for TCSPC measurements and DST, New Delhi, for providing the Single Crystal X-ray Diffractometer facility to the Department of Chemistry, IIT Kharagpur under its FIST program.

References

1 A. Sarkar, A. K. Ghosh, V. Bertolasi and D. Ray, *Dalton Trans.*, 2012, **41**, 1889–1896.
2 N. Zhan, G. Palui, M. Safi, X. Ji and H. Mattoussi, *J. Am. Chem. Soc.*, 2013, **135**, 13786–13795.
3 P. Jiang and Z. Guo, *Coord. Chem. Rev.*, 2004, **248**, 205–229.
4 W. Maret and Y. Li, *Chem. Rev.*, 2009, **109**, 4682–4707.
5 (*a*) M. Irie, *Chem. Rev.*, 2000, **100**, 1683–1684; (*b*) R. Pandey, P. Kumar, A. K. Singh, M. Shahid, P. Li, S. K. Singh, Q. Xu, A. Misra and D. S. Pandey, *Inorg. Chem.*, 2011, **50**, 3189–3197; (*c*) S. A. Ingale and F. Seela, *J. Org. Chem.*, 2012, **77**, 9352–9356.
6 (*a*) E. L. Que, D. W. Domaille and C. J. Chang, *Chem. Rev.*, 2008, **108**, 1517–1549; (*b*) G. Meloni, T. Polanski, O. Braun and M. Vašák, *Biochemistry*, 2009, **48**, 5700–5707; (*c*) S. W. Suh, J. W. Chen, M. Motamedi, B. Bell, K. Listiak, N. F. Pons, G. Danscher and C. J. Frederickson, *Brain Res.*, 2000, **852**, 268–273.
7 (*a*) C. R. Hickenboth, J. S. Moore, S. R. White, N. R. Sottos, J. Baudry and S. R. Wilson, *Nature*, 2007, **446**, 423–427; (*b*) A. L. Garay, A. Pichon and S. L. James, *Chem. Soc. Rev.*, 2007, **36**, 846–855.
8 (*a*) A. Das, G. M. Rosair, M. S. E. Fallah, J. Ribas and S. Mitra, *Inorg. Chem.*, 2006, **45**, 3301–3306; (*b*) S. Sasmal, S. Sarkar, N. Aliaga-Alcalde and S. Mohanta, *Inorg. Chem.*, 2011, **50**, 5687–5695; (*c*) Y.-Q. Wang, Q. Yue, Y. Qi, K. Wang, Q. Sun and E.-Q. Gao, *Inorg. Chem.*, 2013, **52**, 4259–4268; (*d*) A. Escuer, J. Esteban, S. P. Perlepes and T. C. Stamatatos, *Coord. Chem. Rev.*, 2014, **275**, 87–129; (*e*) S. Naiya, S. Biswas, M. G. B. Drew, C. J. Gómez-García and A. Ghosh, *Inorg. Chem.*, 2012, **51**, 5332–5341.
9 (*a*) C.-H. Wang, C.-Y. Li, B.-H. Huang, C.-C. Lin and B.-T. Ko, *Dalton Trans.*, 2013, **42**, 10875–10884; (*b*) A. Erxleben, *Coord. Chem. Rev.*, 2003, **246**, 203–228.
10 (*a*) A.-X. Zheng, J. Si, X.-Y. Tang, L.-L. Miao, M. Yu, K.-P. Hou, F. Wang, H.-X. Li and J.-P. Lang, *Inorg. Chem.*, 2012, **51**, 10262–10273; (*b*) K. A. McCall, C.-c. Huang and C. A. Fierke, *J. Nutr.*, 2000, **130**, 1437S–1446S; (*c*) M. Dey, C. P. Rao, P. Saarenketo, K. Rissanen and E. Kolehmainen, *Eur. J. Inorg. Chem.*, 2002, 2207–2215.
11 Z. He, C. He, Z.-M. Wang, E.-Q. Gao, Y. Liu and C.-H. Yan, *Dalton Trans.*, 2004, 502–504.
12 (*a*) C. Biswas, M. G. B. Drew, E. Ruiz, M. Estrader, C. Diaz and A. Ghosh, *Dalton Trans.*, 2010, **39**, 7474–7484; (*b*) R. Biswas, S. Mukherjee, P. Kar and A. Ghosh, *Inorg. Chem.*, 2012, **51**, 8150–8160.
13 (*a*) Y. Song, Z. Xu, Q. Sun, B. Su, Q. Gao, H. Liu and J. Zhao, *J. Coord. Chem.*, 2008, **61**, 1212–1220; (*b*) S. Mandal, A. K. Rout, A. Ghosh, G. Pilet and D. Bandyopadhyay, *Polyhedron*, 2009, **28**, 3858–3862.
14 X. Li, X. Yang, Y. Li, Y. Gou and Q. Wang, *Inorg. Chim. Acta*, 2013, **408**, 46–52.
15 U. A. Bhagwat, V. A. Mukhedkar and A. J. Mukhedkar, *J. Chem. Soc., Dalton Trans.*, 1980, 2319–2322.
16 (*a*) A. T. R. Williams, S. A. Winfield and J. N. Miller, *Analyst*, 1983, **108**, 1067–1068; (*b*) *Principles of Fluorescence Spectroscopy*, ed. J. R. Lakowicz, Kluwer Academic/Plenum Publishers, NY, 2nd edn, 2003.
17 *Saint, Smart and XPREP*, Siemens Analytical X-ray Instruments Inc., Madison, WI, 1995.
18 G. M. Sheldrick, *SHELXS-97*, University of Göttingen, Göttingen, Germany, 1997.
19 G. M. Sheldrick, *SHELXL 97, Program for Crystal Structure Refinement*, University of Göttingen, Göttingen, Germany, 1997.
20 G. M. Sheldrick, *SADABS: Software for Empirical Absorption Correction*, University of Göttingen, Institute fur Anorganische Chemieder Universitat, Göttingen, Germany, pp. 1999–2003.
21 (*a*) S. Paul, R. Clérac, N. G. R. Hearns and D. Ray, *Cryst. Growth Des.*, 2009, **9**, 4032–4040; (*b*) P. Dhal, M. Nandy, D. Sadhukhan, E. Zangrando, G. Pilet, C. J. Gómez-García and S. Mitra, *Dalton Trans.*, 2013, **42**, 14545–14555.
22 P. B. Chatterjee, S. M. T. Abtab, K. Bhattacharya, A. Endo, E. J. Shotton, S. J. Teat and M. Chaudhury, *Inorg. Chem.*, 2008, **47**, 8830–8838.
23 H. S. Jena and V. Manivannan, *Inorg. Chim. Acta*, 2013, **394**, 210–219.
24 W. A. Addison, T. N. Rao, J. Reedijk, J. V. Rijn and G. C. Verschoor, *J. Chem. Soc., Dalton Trans.*, 1984, 1349–1356.
25 L. Yang, D. R. Powell and R. P. Houser, *Dalton Trans.*, 2007, 955–964.
26 C. L. Dollberg and C. Turro, *Inorg. Chem.*, 2001, **40**, 2484–2485.
27 S. Basak, S. Sen, S. Banerjee, S. Mitra, G. Rosair and M. T. G. Rodriguez, *Polyhedron*, 2007, **26**, 5104–5112.
28 X.-X. Zhou, H.-C. Fang, Y.-Y. Ge, Z.-Y. Zhou, Z.-G. Gu, X. Gong, G. Zhao, Q.-G. Zhan, R.-H. Zeng and Y.-P. Cai, *Cryst. Growth Des.*, 2010, **10**, 4014–4022.
29 A. P. de Silva, H. Q. N. Gunaratne, T. Gunnlaugsson, A. J. M. Huxley, C. P. McCoy, J. T. Rademacher and T. E. Rice, *Chem. Rev.*, 1997, **97**, 1515–1566.
30 (*a*) R. Pandey, P. Kumar, A. K. Singh, M. Shahid, P.-z. Li, S. K. Singh, Q. Xu, A. Misra and D. S. Pandey, *Inorg. Chem.*, 2011, **50**, 3189–3197; (*b*) H.-W. Chiang, Y.-T. Su and J.-Y. Wu, *Dalton Trans.*, 2013, **42**, 15169–15182; (*c*) S. Basak, S. Sen, C. Marschner, J. Baumgartner, S. R. Batten, D. R. Turner and S. Mitra, *Polyhedron*, 2008, **27**, 1193–1200; (*d*) N. J. Williams, W. Gan, J. H. Reibenspies and R. D. Hancock, *Inorg. Chem.*, 2009, **48**, 1407–1415.

31 (*a*) M. Schäferling, M. Wu and O. S. Wolfbeis, *J. Fluoresc.*, 2004, **14**, 561–568; (*b*) Z. Lin, M. Wu, M. Schäferling and O. S. Wolfbeis, *Angew. Chem.*, 2004, **43**, 1735–1738.
32 F. V. Bright and C. A. Munson, *Anal. Chim. Acta*, 2003, **500**, 71–104.
33 J. R. Lakowicz and G. Weber, *Biochemistry*, 1973, **12**, 4171–4179.
34 J. R. Alcala, E. Gratton and F. G. Prendergast, *Biophys. J.*, 1987, **51**, 597–604.